The Methyl/Trifluoromethyl Substitution Effect in Boranes. A Gas-phase Electron Diffraction and Vibrational Study of Bis(dimethylamino)-(trifluoromethyl)borane and Dimethylaminobis(trifluoromethyl)borane†

Reneé Hausser-Wallis and Heinz Oberhammer *
Institut für Physikalische und Theoretische Chemie der Universität, 7400 Tübingen, Federal Republic of Germany
Hans Bürger * **and Gottfried Pawelke**
Anorganische Chemie, FB9, Universität-Gesamthochschule, 5600 Wuppertal, Federal Republic of Germany

The gas-phase structures of $CF_3B(NMe_2)_2$ and $(CF_3)_2BNMe_2$ have been determined by electron diffraction. The vibrational spectra have been recorded by i.r. (gas) and Raman (liquid) and valence force fields have been derived. The following skeletal geometric parameters (r_a values with 3σ uncertainties) have been obtained: for $CF_3B(NMe_2)_2$, B–C = 164.8(8), B–N = 142.2(9), C–N = 145.3(4), C–F = 135.2(3) pm, NBN = 125.5(31), FCF = 105.3(4), and τ_{BN} = 24(3)° (τ_{BN} is the torsional angle around the B–N bond from the planar configuration); for $(CF_3)_2BNMe_2$, B–C = 162.3(4), B–N = 142.5(18), C–N = 145.3(7), C–F = 134.3(2) pm, CBC = 122.2(15), FCF = 106.5(2)°. The B–C bonds in the trifluoromethyl compounds are considerably longer than in the analogous methyl derivatives and this CH_3/CF_3 substitution effect is confirmed by the force constants.

In general, shortening of adjacent bonds is observed if a methyl group which is bonded to a first-row element, X, is replaced by trifluoromethyl. The magnitude of this CH_3/CF_3 substitution effect depends on the electronegativity of X.[1,2] It is largest if X = F, where the C–F bond shortens from FCH_3 [139.2(1) pm][3] to FCF_3 [132.04(4) pm][4] by 7.2 pm and is smaller for less electronegative central atoms. This substitution effect has been rationalized qualitatively by polar interactions.[2] If the adjacent atom X carries a negative net charge, the polar interaction is attractive in the CF_3 derivative and the bond shortens with CH_3/CF_3 substitution ($X^{\delta-}$–$C^{\delta-}H_3$ *vs.* $X^{\delta-}$–$C^{\delta+}F_3$). The reverse effect, *i.e.* lengthening of X–C bonds, has been observed for electropositive second-row atoms X such as Si[5] or P.[6] The recently synthesized CF_3-substituted boron compounds,[7] $CF_3B(NMe_2)_2$ and $(CF_3)_2BNMe_2$, provide the opportunity to extend the study of this CH_3/CF_3 substitution effect to first-row elements which are more electropositive than carbon. In this paper we report a gas-phase electron diffraction study, vibrational spectra, and a normal co-ordinate analysis of the above two compounds. The main interest lies in the distance and strength of the B–CF_3 bonds, relative to B–CH_3 bonds in analogous compounds.

Experimental

The compounds $CF_3B(NMe_2)_2$ and $(CF_3)_2BNMe_2$ were prepared by methods described previously.[7] Infrared and Raman spectra obtained in the gas and liquid phases, respectively, have been reported.[7] For the samples used in the electron diffraction experiment no impurities were detected in the spectra.

The electron diffraction intensities were recorded with the Balzers apparatus at the University of Tübingen at two camera distances (25 and 50 cm).[8] The accelerating voltage was *ca.* 60 kV and the electron wavelength was calibrated with ZnO diffraction patterns. The samples were kept at 20 and 18 °C for the trifluoromethyl and bis(trifluoromethyl) compounds, respectively, and the stainless-steel inlet system and nozzle were at 30 °C for both compounds. The camera pressure never exceeded 10^{-5} mbar during the experiment. Two plates for each compound and camera distance were selected and analyzed by standard procedures.[9] The averaged molecular intensities [$sM(s)$] (M = reduced molecular intensities) for the two compounds in the scattering ranges $0.02 < s < 0.17$ and $0.08 < s < 0.35$ pm^{-1} are presented in Figures 1 and 2 in steps of Δs = 0.002 pm^{-1}.

Vibrational Spectra.—The vibrational spectra of both compounds have been reported and briefly discussed.[7] The i.r. spectrum of $(CF_3)_2BNMe_2$ is shown in Figure 3. Although the actual symmetry of $CF_3B(NMe_2)_2$ is not higher than C_1, the polarization data of the Raman lines are consistent with virtual C_s symmetry. In this case the NC_2 groups are twisted out of the CBN_2 plane in opposite directions. Virtual C_2 symmetry requires that the NC_2 groups are twisted in the same sense and that the CF_3 group is freely rotating. The vibrational spectra of $(CF_3)_2BNMe_2$ suggest either C_{2v} or C_2 symmetry. Both point groups are in agreement with the results of the structural investigations if small rotational barriers about the B–C bonds are assumed. According to the normal co-ordinate analysis the twisting of the NC_2 groups has no significant effect on the vibrational spectra. Therefore, the assignments for $CF_3B(NMe_2)_2$ are based on C_s or 'C_2' symmetry, while the final calculations were performed employing the structural parameters of the electron diffraction investigation. Only skeletal fundamentals with the notation of Table 1 are discussed in some detail. As the mass of the CF_3 group and hence dynamic coupling effects are similar to that of a Br atom, comparison with the vibrational spectra of $BrB(NMe_2)_2$ and Br_2BNMe_2 (obtained in the present investigation and quoted in parentheses throughout for corresponding vibrations) is helpful.

Analysis of $CF_3B(NC_2)_2$. Large $^{10/11}B$ shifts are revealed by ν_1 and ν_{16} at 1 404/1 425 (1 400/1 416) and 1 530/1 552 (1 536/1 555) cm^{-1}. Strong i.r. absorptions at 1 204 (1 212) and 1 148 (1 145) cm^{-1} are assigned to ν_5 and ν_{19}, while the symmetric components ν_4 and ν_{18} are associated with i.r. and Raman features occurring at lower wavenumbers, 903—910 (880—900) cm^{-1}. The vibration ν_6, which has the character of a breathing mode, may be assigned to a Raman line at 565 (563) cm^{-1}. The out-of-plane modes ν_{13} and ν_{14} are mixed, and the component occurring at higher energy was found at 674/696 (686/698) cm^{-1}. A polarized Raman line at 1 280 cm^{-1} and a strong i.r. band near 1 110 cm^{-1} are assigned to ν_2 and ν_3/ν_{17},

† *Non-S.I. units employed:* e ≈ 1.602 × 10^{-19} C, bar = 10^5 Pa.

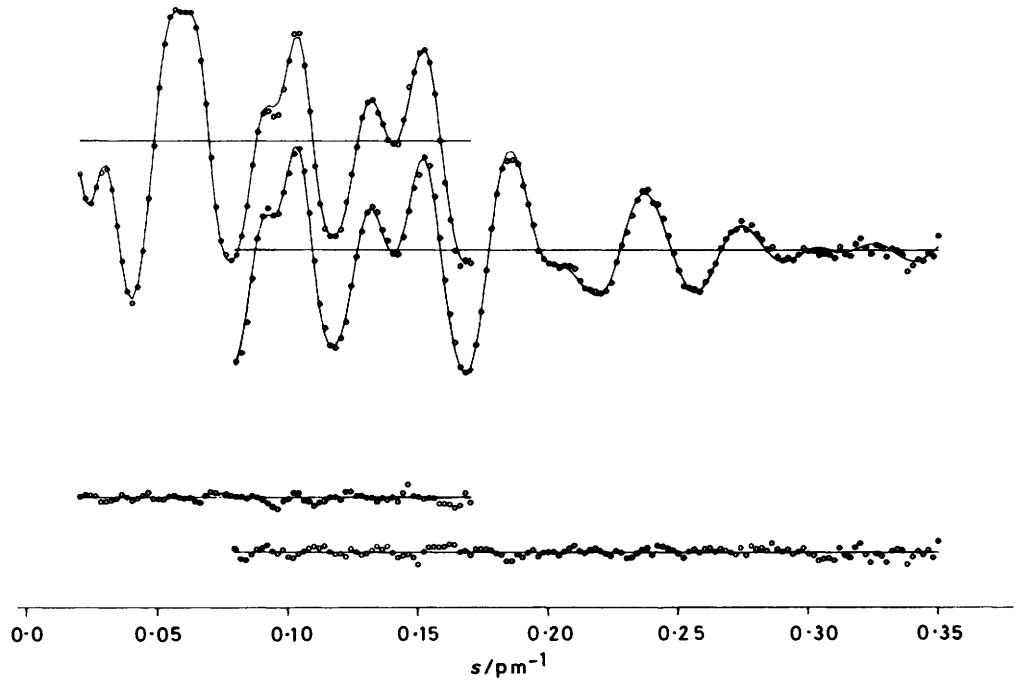

Figure 1. Experimental (points) and calculated (——) molecular intensities [$sM(s)$] and differences for $CF_3B(NMe_2)_2$

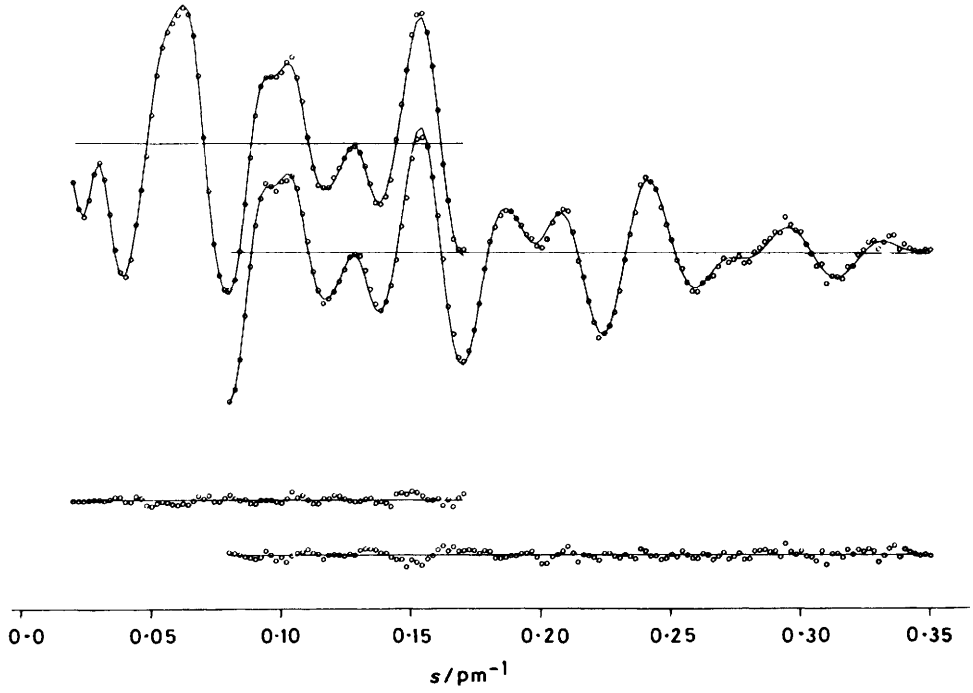

Figure 2. Experimental (points) and calculated (——) molecular intensities [$sM(s)$] and differences for $(CF_3)_2BNMe_2$

respectively, these vibrations being absent in $BrB(NMe_2)_2$. The presence of a CF_3 group is furthermore indicated by a sharp, polarized Raman line at 716 cm^{-1} which is assigned to ν_7, while ν_8 and ν_{20} are associated with an absorption at 515 cm^{-1}. The torsions ν_{15}, ν_{26}, and ν_{27} were not observed. All other skeletal vibrations are strongly mixed, and their assignment requires the assistance of the normal co-ordinate analysis reported below.

Analysis of $(CF_3)_2BNC_2$. The vibration ν_1 is assigned to a strong Raman line coinciding with an i.r. absorption at 1 570/1 600 (1 518/1 532) cm^{-1}, while ν_{24} and ν_4 are located at 1 150 (1 140) and 898/907 (875/885) cm^{-1}, respectively. The b_2 stretch ν_{25} appears as a strong i.r. band with a substantial $^{10/11}B$ shift at 913/935 (833/875) cm^{-1}, while its a_1 counterpart ν_5 is assigned to a polarized Raman line at 292 (315) cm^{-1}. All asymmetric stretching vibrations ν_3, ν_{11}, ν_{16}, and ν_{23} are associated with a broad band in the i.r. and Raman spectrum at

Table 1. Vibrational fundamentals (s = symmetric, asym = asymmetric) for the $CF_3B(NC_2)_2$ (C_s, or 'C_2' in parentheses) and $(CF_3)_2BNC_2$ skeletons (C_{2v})

	$CF_3B(NC_2)_2$		$(CF_3)_2BNC_2$			
	a' (a) (Raman, i.r.)	a'' (b) (Raman, i.r.)	a_1 (Raman, i.r.)	a_2 (Raman)	b_1 (Raman, i.r.)	b_2 (Raman, i.r.)
ν(BN)	ν_1	ν_{16}	ν_1			
$\nu_s(CF_3)$	ν_2		ν_2			ν_{22}
$\nu_{asym}(CF_3)$	ν_3	ν_{17}	ν_3	ν_{11}	ν_{16}	ν_{23}
$\nu_s(NC_2)$	ν_4	ν_{18}	ν_4			
$\nu_{asym}(NC_2)$	ν_5	ν_{19}				ν_{24}
ν(BC)	ν_6		ν_5			ν_{25}
$\delta_s(CF_3)$	ν_7		ν_6			ν_{26}
$\delta_{asym}(CF_3)$	ν_8	ν_{20}	ν_7	ν_{12}	ν_{17}	ν_{27}
$\rho(CF_3)$	ν_9	ν_{21}	ν_8	ν_{13}	ν_{18}	ν_{28}
$\delta(NC_2)$	ν_{10}	ν_{22}	ν_9			
$\delta(BN_2)$	ν_{11}					
δ(BNC)	ν_{12}	ν_{23}				ν_{29}
δ(CBN)		ν_{24}				ν_{30}
$\delta(BC_2)$			ν_{10}			
op(B)*	ν_{13}				ν_{19}	
op(N)*	ν_{14}	ν_{25}			ν_{20}	
τ(BN)	ν_{15}	ν_{26}		ν_{14}		
$\tau(CF_3)$		ν_{27}		ν_{15}	ν_{21}	

* op = Out of plane.

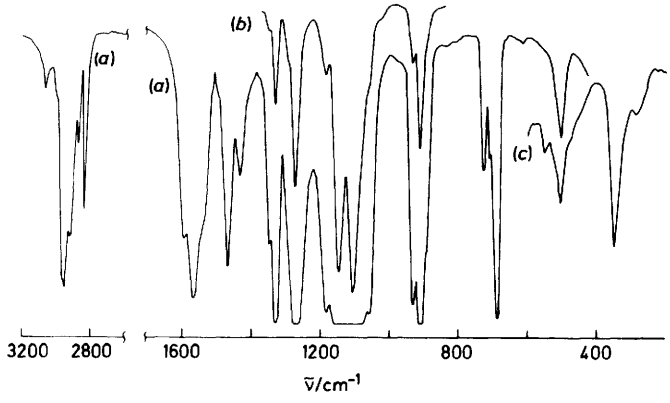

Figure 3. Infrared spectrum of $(CF_3)_2BNMe_2$ (18-cm cell): (*a*) 34 mbar, KBr windows; (*b*) 1.5 mbar, KBr windows; (*c*) 34 mbar, Polythene windows

1 100—1 110 cm^{-1}. The symmetric modes ν_2 and ν_{22} are assigned to vibrations at 1 270 and 1 334/1 344 cm^{-1}. In this region, Br_2BNMe_2 does not show any absorptions. The presence of two CF_3 groups follows from the occurrence of two $\delta_s(CF_3)$ modes, ν_6 at 729 and ν_{26} at 689 cm^{-1}. While ν_{14} may be associated with a weak and broad Raman line near 100 cm^{-1}, the other bending fundamentals were either not detected (*e.g.* ν_{15} and ν_{21}) or, according to the results of the normal co-ordinate analysis, were strongly mixed.

Normal Co-ordinate Analysis.—In order to establish the assignment of the skeletal vibrations, we have performed a normal co-ordinate analysis. Wilson's FG matrix method was employed and the computer program NORCOR applied.[10] The G matrices were based on the structures determined in the present studies. The CH stretching and bending vibrations were excluded from the computations, and the carbon atoms of the CH_3 groups were assigned a mass of 15. Initial force constants were transferred from $CF_3BF_3^-$,[11] $(CF_3)_2BF_2^-$,[12] and $(CH_3)_2NH$[13] and refined to an acceptable fit of the observed vibrational wavenumbers. Tables 2 and 3 give the observed and calculated wavenumbers and quote the respective potential energy distribution in terms of inner co-ordinates. The diagonal force constants are listed in Table 4.*

It is evident that the $^{10/11}B$ shifts of the BN stretching vibrations are poorly reproduced by our calculations, the calculated shifts being significantly larger. The reason for this discrepancy is mainly the mixing of ν_1 and ν_{16} with the CH_3 bending vibrations, which are close, but which were not considered in the calculations. Therefore some of the off-diagonal elements of the F matrix could not be determined. Nevertheless, the assignment of the skeletal vibrations appears to be well founded. The stretching force constants listed in Table 4 are consistent with values of related molecules, *e.g.* f(BN) of $B(NMe_2)_3$, *ca.* 550,[14] f(CN) of NMe_3, 530,[15] and f(BC) and f(CF) of $CF_3BF_3^-$, 363 and 485 N m^{-1},[11] respectively.

Structure Analysis.—The radial distribution functions (Figures 4 and 5) were calculated with an artificial damping constant, $\gamma = 19$ pm^2. In the least-squares analyses the molecular intensities were modified with a diagonal weight matrix[9] and scattering amplitudes and phases from ref. 16 were used. In both compounds C_{3v} symmetry for the CF_3 and CH_3 groups and a planar configuration of the dimethylamino groups was assumed. Planarity of $-NH_2$ and $-NMe_2$ groups bonded to boron has been demonstrated by *ab initio* calculations[17,18] and experiments.[19-22] The methyl groups were assumed to deviate slightly from the exact staggered position (with respect to the B–N bond). The torsional angle around the N–C bonds was set to 10°, the value derived for $B(NMe_2)_3$,[22] with the two CH_3 groups rotated in opposite directions (*i.e.* C_2 symmetry for $-NMe_2$). A value of $\tau_{NC} = 0$ corresponds to the position with two C–H bonds staggering the B–N bond. Test calculations demonstrated that this torsional angle has only a small effect on the quality of the fit between experiment and model and does not affect the optimized structural parameters.

Structure of $CF_3B(NMe_2)_2$. With the above constraints the geometry of this compound is characterized by five bond

* Complete force field data are available on request from H. B.

Table 2. Observed and calculated vibrational wavenumbers (cm^{-1}) for the $CF_3B(NC_2)_2$ skeleton with their potential energy distribution in terms of internal co-ordinates (only contributions ≥ 10%) (op = out of plane)

$^{11/10}B$														
Observed	Calculated	BC	BN	NC	CF	CBN	NBN	BNC	CNC	BCF	FCF	op(N)	op(B)	τ(BN)
1 530/1 552	1 515/1 569		88			17								
1 404/1 425	1 400/1 438	23	35	19			16	19						
1 280	1 280	26	16		27					12	25			
1 204	1 200			77	17									
1 148	1 144/1 149		18	76										
1 110	1 123			32	66						18			
1 108	1 100/1 102				96					16	26			
907/920	912/917			93										
903/907	903/905			98										
716	716				36						16			
674/696	676/699				15			18		19			34	
565	567/568		40				12	39	36					
563	559/560				29	11		15	22		11			
515	519				20						77			
512	507							12	19		66			
385	387	27						25	18		12			
380	376							70	17	20				
345	350							23	42	32				
340	335									42		28	12	
290	299							36	37			24		
285	280	19						23	15			40		
175	160					43		29		15				
135	135											56	39	
135	129					21	36	41				28		
	78													96
	75													97

Table 3. Observed and calculated vibrational wavenumbers (cm^{-1}) for the $(CF_3)_2BNC_2$ skeleton with their potential energy distribution in terms of internal co-ordinates (only contributions ≥ 10%) (op = out of plane)

Symmetry	$^{11/10}B$														
	Observed	Calculated	BC	BN	NC	CF	CBN	BNC	CNC	CBC	BCF	FCF	op(N)	op(B)	τ(BN)
a_1	1 570/1 600	1 560/1 609		38		13				20	11				
	1 270	1 269/1 272	24	12		41						22			
	1 110	1 110/1 112		29	18	46						21			
	898/907	890/905			81	24									
	729	727				41						14			
	564	565		31		31			26			16			
	495	494		22				16	60			52			
	350	351			17			13	51		16	27			
	292	292	35				15					25			
	138	138					14			34	100				
a_2	1 090	1 088				107					11	25			
	528	526				17						73			
	275	273									106	20			
	101	101													98
b_1	1 110	1 118/1 122				95					17	23			
	690/710	688/709				25					24		13	31	
	505	505/506										82			
	351	351/353									46	13	56		
	138	136									32		25	63	
b_2	1 334/1 344	1 332/1 347	15		48	10	30	13							
	1 150	1 146/1 154	50		28	29					10	19			
	1 106	1 107	14			77					11	25			
	913/935	914/934	24			47	16								
	689	689/691				25					13	28			
	520	523				16						75			
	348	346	45					33				10			
	270	275						15			88	20			
	138	139					45	64			19				

Table 4. Diagonal inner force constants (N m^{-1} scaled to 100 pm) for the $CF_3B(NC_2)_2$ and $(CF_3)_2BNC_2$ skeletons

	$CF_3B(NC_2)_2$	$(CF_3)_2BNC_2$
f(BC)	355	360
f(BN)	600	600
f(NC)	520	520
f(CF)	485	490
f(CBN)	134	159
f(CBC)		186
f(NBN)	116	
f(BNC)	107	74
f(CNC)	101	139
f(BCF)	115	98
f(FCF)	194	174
f_{op}(B)	25	31
f_{op}(N)	12	26
f_t(BN)	14	24

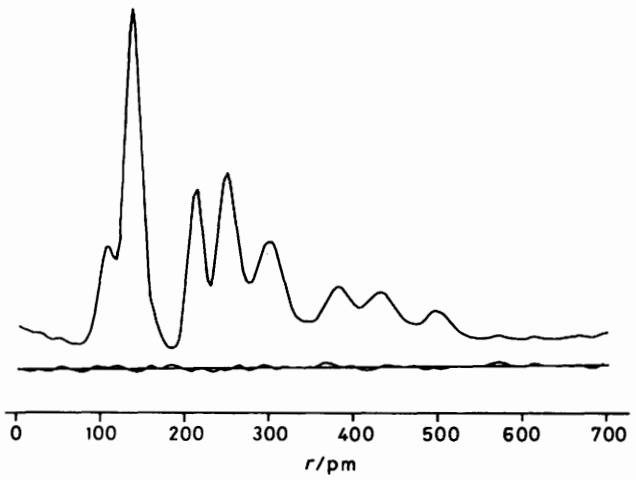

Figure 4. Experimental radial distribution function and difference curve for $CF_3B(NMe_2)_2$

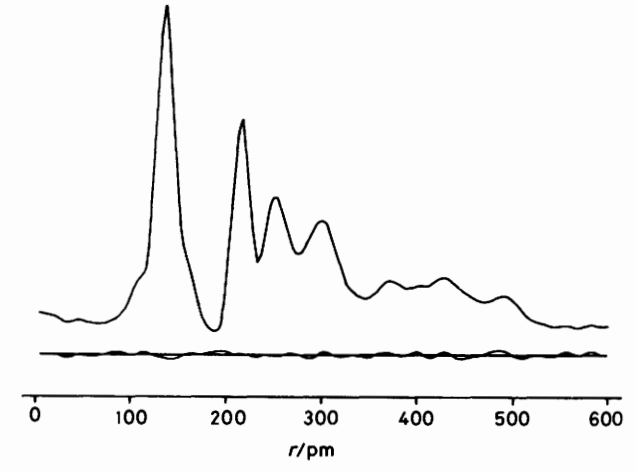

Figure 5. Experimental radial distribution function and difference curve for $(CF_3)_2BNMe_2$

lengths, four bond angles (HCH, FCF, CNC, and NBN) and the torsional angles τ_{BN}, by which the dimethylamino groups are rotated around the B–N bonds from the planar configuration (Figure 6). The two $-NMe_2$ groups are rotated in opposite directions resulting in C_2 symmetry for the $B(NMe_2)_2$ moiety.

Table 5. Geometric parameters[a] for $CF_3B(NMe_2)_2$ and $(CF_3)_2BNMe_2$

	$CF_3B(NMe_2)_2$	$(CF_3)_2BNMe_2$
B–C	164.8(8)	162.3(4)
B–N	142.2(9)	142.5(18)
C–N	145.3(4)	145.3(7)
C–F	135.2(3)	134.3(2)
C–H	109.3(5)	107.9(9)
NBN	125.5(31)	
CBC		122.2(15)
CNC	114.6(19)	110.7(37)
FCF	105.3(4)	106.5(2)
HCH	109.2(11)	108.9(14)
τ_{NC}[b]	10[c]	10[c]
τ_{BN}[d]	24(3)	0[c]
τ_{BC}[e]	f	15.1(11)

[a] r_a Values, bond lengths in pm and angles in °. Estimated uncertainties are 3σ values and include possible systematic errors (see text). [b] Torsional angle around NC bonds; for $\tau_{NC} = 0$ two CH bonds stagger the BN bond. [c] Not refined. [d] Torsional angle around the BN bond; $\tau_{BN} = 0$ corresponds to the planar heavy-atom skeleton. [e] Torsional angle around the B–C bonds; for $\tau_{BC} = 0$ two CF bonds stagger the BN bond. [f] Free internal rotation of CF_3 group.

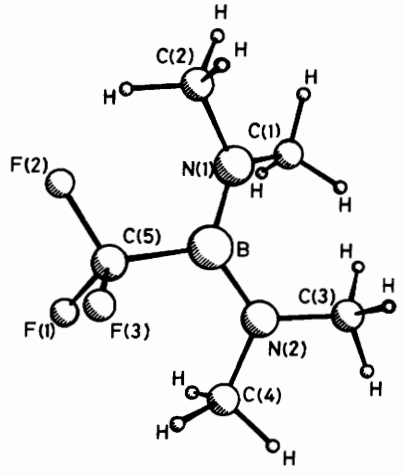

Figure 6. Molecular model of $CF_3B(NMe_2)_2$ with atomic numbering

The radial distribution function in the range $260 < r < 350$ pm is very sensitive towards the torsional position of the CF_3 group. The initial assumption of $\tau_{BC} = 0$, *i.e.* one C–F bond perpendicular to the molecular plane, leads to poor agreement between experiment and model. The experimental intensities can be fitted almost equally well with a rigid model and an 'effective' torsional angle for the CF_3 group $\tau_{BC} = 31(5)°$ or with a non-rigid model with free internal rotation of the CF_3 group. This torsional potential has six fold symmetry and such potentials are known to have very low barriers.

For both models the geometric parameters agree within their standard deviations and the values in Table 5 correspond to the non-rigid analysis. The vibrational amplitudes were grouped according to their distances and constraints are evident from Table 6. Amplitudes for distances involving hydrogens were not refined. With these assumptions ten geometric parameters and ten vibrational amplitudes were refined simultaneously in the final analysis. The following correlation coefficients had values larger than |0.6|: CF/BN, −0.75; CF/NC, 0.75; BN/NC, −0.92; CF/FCF, 0.88; BN/FCF, −0.71; NC/FCF, 0.68. The estimated uncertainties in Tables 5 and 6 are based on 3σ values and include possible systematic errors due to the constraints for

Table 6. Interatomic distances and vibrational amplitudes (pm) for $CF_3B(NMe_2)_2$ (excluding distances involving hydrogens)[a]

Atom pair	Distance	Amplitude	Atom pair	Distance	Amplitude
C–H	109	6.9(5)	N···F	284—311	19(6)
C–F	135	4.9[b]	C···F	258—329	12(3)
B–N	142	4.7[b]	C(2)···C(5)	302	11(3)
N–C	145		C(1)···C(3)	307	
B–C	165		N(1)···C(3)	307	
F···F	215	5.8(3)	N···F	357—378	16(6)
C(1)···C(2)	245	8.7(5)	C(1)···C(4)	382	10(2)
B···F	251		C(1)···C(5)	396	
B···C(1)	252		C···F	412—471	11(4)
N···N	253		C···F	493—501	10(3)
N···C(5)	262		C(2)···C(5)	505	

[a] Atom numbering is shown in Figure 6. Error limits are 3σ values. [b] Not refined.

Table 7. Interatomic distances and vibrational amplitudes (pm) for $(CF_3)_2BNMe_2$ (excluding distances involving hydrogens)[a]

Atom pair	Distance	Amplitude	Atom pair	Distance	Amplitude
C–H	108	7.4(12) (l_1)	N···F(1)	320	17(5) (l_7)
C–F	134	4.9(2) (l_2)	C(3)···F(1)	333	
B–N	143	4.7[b]	C(2)···F(1)	365	16(3) (l_8)
N–C	145		F(2)···F(4)	367	
B–C	162	4.1(9) (l_3)	N···F(2)	375	17(5) (l_9)
F···F	215	6.2(2) (l_4)	C(2)···F(3)	385	
C(3)···C(4)	239	7.9(11) (l_5)	F(3)···F(5)	419	14(3) (l_{10})
B···F	247		F(3)···F(4)	435	21(4) (l_{11})
B···C(3)	255		C(3)···F(2)	435	
C(1)···C(2)	284		C(3)···F(6)	439	
F(2)···F(5)	265	12[b]	C(3)···F(4)	456	24(8) (l_{12})
C(3)···F(3)	288	12(2) (l_6)	F(1)···F(4)	470	
N···F(3)	298		F(3)···F(6)	491	11(3) (l_{13})
C(1)···F(5)	302		C(3)···F(5)	500	
C(1)···C(3)	304	10[b]			
C(2)···C(3)	401				

[a] Atom numbering is shown in Figure 7. Error limits are 3σ values. [b] Not refined.

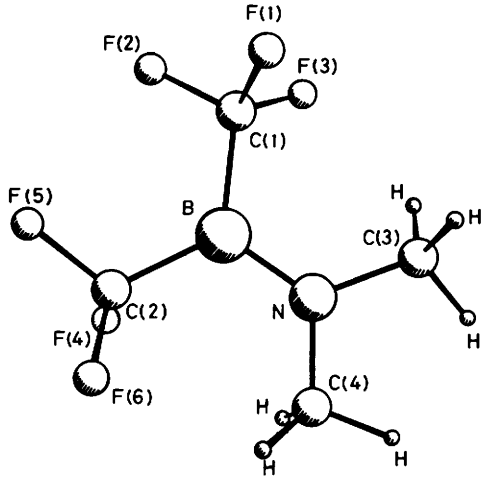

Figure 7. Molecular model of $(CF_3)_2BNMe_2$ with atomic numbering

bonded vibrational amplitudes. These systematic errors were estimated by varying these amplitudes by ±0.5 pm.

Structure of $(CF_3)_2BNMe_2$. Model calculations demonstrate that the heavy-atom skeleton (without fluorines) is planar or nearly planar (Figure 7). Thus, in addition to the geometric constraints described above, the torsional angle around the B–N bond was set to zero. Since the choice of the model, rigid or non-rigid, had no effect on the fit or on the values for the geometric parameters in the case of $CF_3B(NMe_2)_2$, only a rigid model was used for $(CF_3)_2BNMe_2$. For compounds with two or more large-amplitude motions (CF_3 torsions in this case) non-rigid models increase the computational expense drastically. The CF_3 groups were assumed to be rotated around the B–C bonds (τ_{BC}) in opposite directions, resulting in C_2 overall symmetry. These torsional angles have to be considered as 'effective' values. Constraints for the vibrational amplitudes are evident from Table 7. With these assumptions ten geometric parameters and 13 vibrational amplitudes were refined simultaneously. The following correlation coefficients had values larger than |0.6|: BN/NC, −0.80; BN/CNC, 0.62; CBC/CNC, −0.72; BN/l_2, 0.63; CBC/l_9, 0.63; CBC/l_{11}, 0.66. The final results are listed in Tables 5 and 7. The uncertainties have been estimated by the same procedure as described above.

Results and Discussion

The most interesting structural parameter in these CF_3-substituted boranes is the B–C bond lengths. Comparison with the analogous CH_3 derivatives,[23] $CH_3B(NHMe)_2$ and $(CH_3)_2BNHMe$, demonstrates considerable lengthening of these bonds upon CH_3/CF_3 substitution: from 158.6(3) to 164.8(8) pm in the methylborane and from 158.6(2) to 162.3(4) pm in the dimethylborane. A similar effect has been observed previously in the crystal structures of the borates $K[CH_3BF_3]$[24] and $K[CF_3BF_3]$[11] where the B–C bond lengthens from 157.5(3) to 162.5(5) pm. The observation of longer B–C bonds in the CF_3 derivatives relative to BMe_3 [B–C = 157.8(2) pm][25] is consistent with the f(BC) stretching force constants which

decrease from 384 N m^{-1} in BMe_3[26] to 355 and 360 N m^{-1} in the CF_3 compounds.

The lengthening of the B–C bonds with fluorination is in agreement with the simple concept of polar interactions. Since the electropositive boron atom carries a positive net charge, the polar interaction changes from slightly attractive in the methyl compounds (methyl carbon is assumed to carry a small negative net charge) to strongly repulsive in the CF_3 derivatives. If polar effects are indeed dominant in determining the B–CF_3 bond lengths, the difference between $(CF_3)_2BNMe_2$ [162.3(4) pm] and $CF_3B(NMe_2)_2$ [164.8(8) pm] indicates stronger repulsion, *i.e.* a higher positive boron net charge in the latter compound. Such an increase in the boron net charge with an increasing number of amino groups has been predicted by *ab initio* calculations[27] on H_2BNH_2 (q_B = +0.36 e) and $HB(NH_2)_2$ (q_B = +0.70 e), but is not obvious for the CF_3-substituted compounds. The slightly, but significantly longer C–F bonds in $CF_3B(NMe_2)_2$, however, are consistent with a higher positive net charge in this compound.

The correlation between C–F bond lengths in CF_3 groups and the electronegativity or net charge of the adjacent atom, *i.e.* lengthening with increasing positive net charge, has been established previously.[2,28] The C–F bonds in the boron compounds are long but typical for CF_3 groups bonded to electropositive atoms [*e.g.* 134.8(1) pm in CF_3SiH_3[5] or 135.4(2) pm in CF_3HgCH_3[29]]. The FCF angles [105.3(4) and 106.5(2)°] are considerably smaller than tetrahedral but are in perfect agreement with a previously established correlation between these angles and the C–F bond lengths:[2,28] the FCF angles decrease with increasing C–F bond lengths, resulting in remarkably constant non-bonded F ··· F distances of 215 ± 1 pm. These F ··· F distances are 215.0(6) and 215.2(4) pm in $CF_3B(NMe_2)_2$ and $(CF_3)_2BNMe_2$, respectively.

The remaining geometric parameters are not affected by fluorination. The B–N and N–C bond lengths are equal in both CF_3 derivatives and within experimental uncertainties they are equal to the corresponding values in other dimethyl- or methylaminoboranes. The only exception is the B–N bond in Me_2BNHMe of 139.4(2) pm.[23]

Acknowledgements

Financial support by the Fonds der Chemischen Industrie is gratefully acknowledged.

References

1 A. Yokozeki and S. H. Bauer, *Top. Curr. Chem.*, 1975, **53**, 71.
2 H. Oberhammer, *J. Fluorine Chem.*, 1983, **23**, 147.
3 K. Oyanagi and K. Kuchitsu, Seventh Austin Symposium on Gas Phase Molecular Structure, Austin, Texas, 1978, paper A15.
4 M. Fink, C. W. Schmiedekamp, and D. J. Gregory, *Chem. Phys.*, 1979, **71**, 5238.
5 H. Beckers, H. Bürger, R. Eujen, B. Rempfer, and H. Oberhammer, *J. Mol. Struct.*, 1986, **140**, 281.
6 C. J. Marsden and L. S. Bartell, *Inorg. Chem.*, 1976, **15**, 2713.
7 H. Bürger, M. Grunwald, and G. Pawelke, *J. Fluorine Chem.*, 1986, **31**, 89.
8 H. Oberhammer, in 'Molecular Structures by Diffraction Methods,' The Chemical Society, London, 1976, vol. 4, p. 24.
9 H. Oberhammer, H. Willner, and W. Gombler, *J. Mol. Struct.*, 1981, **70**, 273.
10 D. Christen, *J. Mol. Struct.*, 1978, **48**, 101.
11 D. J. Brauer, H. Bürger, and G. Pawelke, *Inorg. Chem.*, 1977, **16**, 2305; *J. Chem. Phys.*, 1965, **42**, 3076.
12 D. J. Brauer, H. Bürger, and G. Pawelke, *J. Organomet. Chem.*, 1980, **192**, 305.
13 A. Y. Hirakawa, M. Tsuboi, and T. Shimanouchi, *J. Chem. Phys.*, 1972, **57**, 1236.
14 H. J. Becher, *Z. Anorg. Allg. Chem.*, 1956, **287**, 285.
15 B. Beagley and A. R. Medwid, *J. Mol. Struct.*, 1977, **28**, 229.
16 J. Haase, *Z. Naturforsch., Teil A*, 1970, **25**, 936.
17 O. Gropen and H. M. Seip, *Chem. Phys. Lett.*, 1974, **25**, 206.
18 J. D. Dill, P. v. R. Schleyer, and J. A. Pople, *J. Am. Chem. Soc.*, 1975, **97**, 3402.
19 M. Sugie, H. Takeo, and C. Matsumura, *Chem. Phys. Lett.*, 1979, **64**, 573.
20 L. R. Thorne and W. D. Gwinn, *J. Am. Chem. Soc.*, 1982, **104**, 3822.
21 F. B. Clippard and L. S. Bartell, *Inorg. Chem.*, 1970, **9**, 2439.
22 A. H. Clark and G. A. Anderson, *Chem. Commun.*, 1969, 1082.
23 A. Almenningen, G. Gundersen, M. Mangerud, and R. Seip, *Acta Chem. Scand., Ser. A*, 1981, **35**, 341.
24 D. J. Brauer, H. Bürger, and G. Pawelke, *J. Organomet. Chem.*, 1982, **238**, 267.
25 L. S. Bartell and B. L. Carrol, *J. Chem. Phys.*, 1965, **42**, 3076.
26 H. J. Becher and F. Bramsiepe, *Spectrochim. Acta, Part A*, 1979, **35**, 53.
27 T. Fjeldberg, G. Gundersen, T. Jonvik, H. M. Seip, and S. Saebo, *Acta Chem. Scand., Ser. A*, 1980, **34**, 547.
28 V. Typke, M. Dakkouri, and H. Oberhammer, *J. Mol. Struct.*, 1978, **44**, 85.
29 H. Günther, H. Oberhammer, and R. Eujen, *J. Mol. Struct.*, 1980, **64**, 249.

Received 8*th August* 1986; *Paper* 6/1621